DAMIANO ZITO
Progold S.p.a.
Trissino (VI)

Damiano Zito is the CEO for Progold S.p.A. in Trissino, Italy. He is a board member of Italian Jewellery Association as delegate for Norms and Innovation. He has 25 years of experience in the field. He is a recipient of the Santa Fé Symposium Ambassador Award and his company's R&D Department is a two-time winner of the Research Award.

This paper is a development of the results presented at the 2012 Santa Fe Symposium®. The effect of the most representative variables of the Selective Laser Melting (SLM) technology on the quality of final products is evaluated by means of the design of experiment approach (DOE). The variables taken into account are laser power, scanning speed and thickness of the powder layer. The aim of this paper is to identify the chemical-physical characteristics of the powder that ensure the best results of the SLM technique. Analysis of the influence of chemical composition and powder particle size distribution on porosity and roughness of the final items is specifically studied. This work describes the progress obtained with SLM technology in the last year, and evidences the importance of optimising process parameters. All presented results were obtained using precious metal alloys.

Optimisation of the Main Selective Laser Melting Technology Parameters in the Production of Gold Jewellery

Damiano Zito(a), Alessio Carlotto(a), Alessandro Loggi(a), Dr. Patrizio Sbornicchia(a), Daniele Maggian(a), Dr. Matthias Fockele(b), Peter Unterberg(b), Prof.Alberto Molinari(c), Prof. Ilaria Cristofolini(c)

(a) Progold S.p.A, Trissino (VI), Italy
(b) Realizer GMBH, Borchen, Germany
(c) Università degli Studi di Trento, Trento (TN), Italy

Abstract
This paper is a development of the results presented at the 2012 Santa Fe Symposium®. The effect of the most representative variables of the Selective Laser Melting (SLM) technology on the quality of final products is evaluated by means of the design of experiment approach (DOE). The variables taken into account are laser power, scanning speed and thickness of the powder layer. The aim of this paper is to identify the chemical-physical characteristics of the powder that ensure the best results of the SLM technique. Analysis of the influence of chemical composition and powder particle size distribution on porosity and roughness of the final items is specifically studied. This work describes the progress obtained with SLM technology in the last year, and evidences the importance of optimising process parameters. All presented results were obtained using precious metal alloys.

Introduction
Former experimental work on Selective Laser Melting (SLM) showed the effect of particle size distribution in the alloy powder and the effect of laser parameters on surface quality and mechanical properties of the produced items [1, 2] . The general trend showed that a higher laser specific energy causes higher density of the produced items along with a higher mechanical strength and a lower surface roughness, while scanning speed and particle size distribution show a lower effect on alloy density. Moreover surface roughness decreased with increased surface tilt angle. Therefore the surfaces with higher tilt angle from the work surface show lower roughness. Grain size is fine and practically independent from building parameters. Therefore mechanical strength is higher than in items produced with traditional or direct investment casting. “Traditional” casting denotes the process including wax injection in a rubber mould. “Direct” casting refers to the process where wax injection is replaced by resin or wax models produced with RP methods, also for manufacturing.

In this work we deal with the effect of chemical composition of alloy powder and with the effect of typical laser parameters on optical and mechanical properties of the produced items. More specifically, a standard gold-silver-copper alloy has been compared with an alloy containing an addition able to markedly reduce surface tension, such as gallium. A further experimentation has been carried out with the same gold-silver-copper alloy, but with a different powder particle size range. We also intended to evaluate how the results of the SLM process depend on particle size range in the alloy powder, that causes different apparent density and flow properties.

Experimental practice

Alloy items have been built with a SLM 50 (Realizer) machine equipped with a fibre laser (100W) having a 10 µm spot and with a circular work table (70 mm diameter) placed in a chamber under an argon protective atmosphere. The alloy powder was produced in our laboratories with a gas atomizer, working in an environment fully protected with inert gas at atmospheric pressure.

The shape of the produced alloy powders has been controlled in our laboratories by electron microscopy. The particle size distribution has been controlled with a Malvern laser granulometer (Hydro 2000S).
The gas atomisation process enables to obtain humidity free powders with spherical, not agglomerated particles, with a narrow particle size range, that are well suited for SLM (Figures 1 and 2). Particle shape and humidity content are important because of their effect on powder flow under the distributing blade on the working platform. The evaluation of powder flowability has been carried out with a Hall Flowmeter Funnel (ASTM B 213-03) and with a Carney Flowmeter Funnel (ASTM B 417-89). Apparent density was measured with a standard volume cup (ASTM B 212, B 329 and B 417).

Chemical composition of the alloy powders has been selected in order to obtain a significant variation of surface tension of the liquid metal, of thermal conductivity and surface reflectivity in comparison with the standard ternary alloy (Table 1). Grain refining additions are not necessary in alloys for SLM, because a fine grain size is a consequence of this process. The addition of low boiling point elements, such as zinc, was avoided, to reduce gas porosity.

ALLOY	Au (‰)	Ag (‰)	Cu (‰)	Ga (‰)	Powder particles size range (µm)
1	752	40	208	0	0-53
2					5-53
3	752	40	188	20	0-53

Table 1 – Chemical composition of the alloys used for Selective Laser Melting (SLM)

The powder with 5-53 µm particle size range was obtained from a powder with 0-53 µm particle size range. The particles in the 0-5 µm size range were removed with an Hosokawa Alpine (100 MZR) classifier. This equipment enables to selectively remove the particles in a given size range as a function of air flow rate and rotation rate of the turbine.

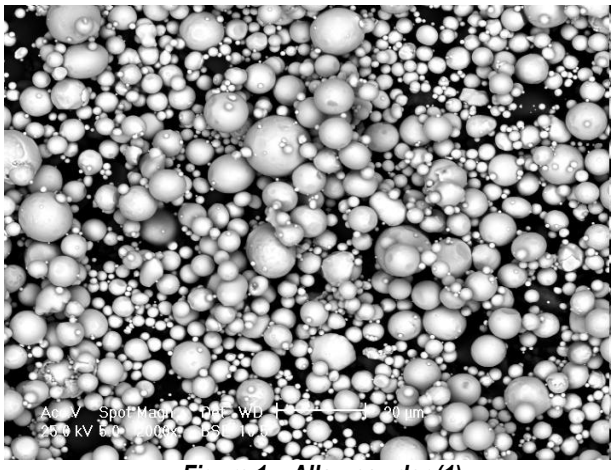

Figure 1 – Alloy powder (1)

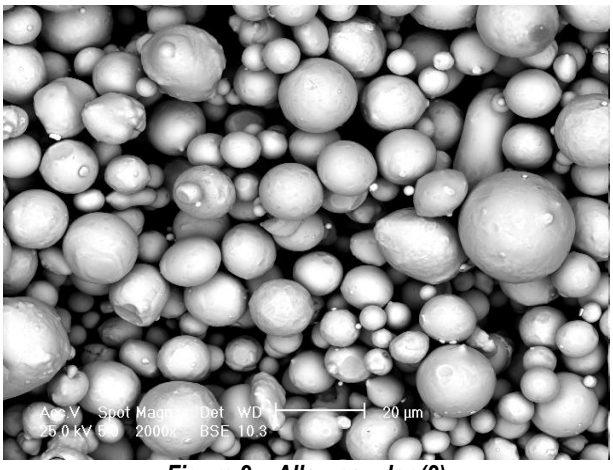

Figure 2 – Alloy powder (2)

Surface evaluation of raw produced pieces has been carried out with a stereoscopic optical microscope, optical and electronic metallography and with a Taylor Hobson profilometer (Form Talysurf Intra2) equipped with a carbon fibre feeler pin with a 2.0 µm radius diamond tip.
Porosity was evaluated with the software Leica Qwin (Leica Microsystems). The experimental pieces were designed with the McNeel software (Rhinoceros 4.0) and the support structure was added with Materialise software (Magics 16.02).
The experimental pieces had the shape of a rectangular parallelepiped (l = 10.00 mm, h = 5.00 mm) having inner lamellar structure with a uniform 500 µm nominal gap width. However the real gap width among the thin plates and their real thickness depend on the laser power and on the scanning speed (Figures 3 and 4): The thin plates are named vectors and each of them was produced with a single laser pass for each prototyping stage. The microstructural inspections aimed to evaluate the effect of the laser parameters on the efficiency of powder melting and to find the conditions for maximizing densification and minimizing porosity. The quality of the produced specimens has been evaluated for different laser power levels, point distance in outer wall and hatches and pulse duration on the alloy powder bed (Table 2).

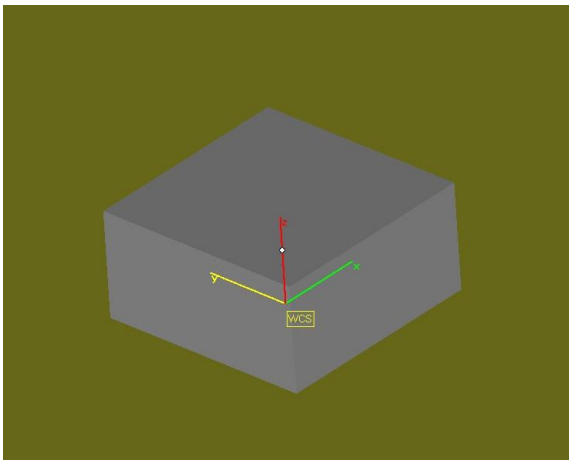

Figure 3 – Model of the rectangular parallelepiped

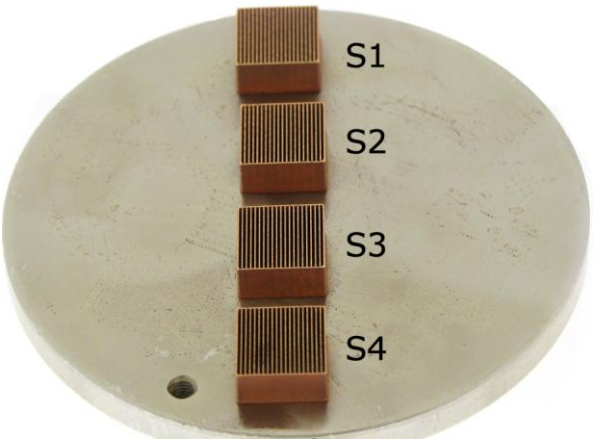

Figure 4 – Set of rectangular parallelepipeds as obtained with Magics (Materialise)

The first set of experiments (S1 - S4) has been carried out with a fixed scanning speed and the laser power has been varied from 92.5 kW to 62.5 kW with 10 W steps (Table 2). The distance of the laser spots on the outer wall of the specimens (30 µm) was appreciably lower in comparison with the distance of the laser spots on the inner vectors (40 µm), for obtaining a thicker outer shell with higher strength for the evaluation of the specimens, that in our case have a lamellar structure. The second (S5 - S8) and the third (S9 – S12) set of experiments have been carried out with laser power similar to the first set, but with different scanning speed.

To compare the SLM technique with the present jewellery production techniques, the same specimens have been produced with investment casting, starting from injected wax models or from resin prototyped models (3D System). The following procedure was used:

1) Pre-melting in an induction heated casting machine. Alloy ingots were cast from a temperature 150°C higher than the liquidus temperature. The ingots were rolled and cut to facilitate the subsequent production steps.

2) Melting has been carried out under vacuum in an induction heated casting machine. Casting temperature was 150°C higher than liquidus temperature. Flask temperature was 550°C with five minutes holding time in the machine after casting. Then the flasks were subjected to fast cooling in water.

Results and discussion

In the first set of experiments (S1 to S4) reducing laser power causes thinning of the vectors (Figures 5, 6, 7, 8) because the volume of melted alloy is reduced, along with the time for solidification of the molten metal. However scanning speed is sufficiently low for producing a good continuity of the vector profile. Therefore the thin plates show a rather linear and uniform contour. This advantage is lost in the second set of experiments (S5 to S8), where the scanning speed of the laser is increased from 0,33 m/s to 0,50 m/s, other conditions being the same (Figures 9, 10, 11, 12).
The increased scanning speed along with the reduced laser power prevents a continuous and linear melting of a sufficient volume of alloy powder, increases the length of the liquid spot and causes instability phenomena [3]. So vectors are grown with a more undulated, irregular contour.
By definition,the scanning speed is given by the ratio between the distance between the spots (d_{spot}) and the exposure time t_e (eqn.1), but we can have different results for vectors quality for the same scanning speed if we change the distance between the spots or the exposure time. The effect of the distance between the spots turned out to be more important than the exposure time: with the same scanning speed a decrease of the distance between the laser spots increases the linearity of the vectors appreciably, even if the laser exposure time has been proportionally reduced (Figures 13, 14, 15, 16). This happens because a shorter distance between the spots causes a better continuity of the molten alloy bath. On the contrary a longer distance can induce a partial interruption of the vector and the contour of the lamellae is more indented.

Test id. number	Power (W)	Exposure (µs)	Spot distance on the Contour (µm)	Spot distance on the Vectors (µm)	Scanning speed on the Contour (m/s)	Scanning speed on the Vectors (m/s)
S1	92,5	120	30	40	0,25	0,33
S2	82,5	120	30	40	0,25	0,33
S3	72,5	120	30	40	0,25	0,33
S4	62,5	120	30	40	0,25	0,33
S5	92,5	120	50	60	0,42	0,50
S6	82,5	120	50	60	0,42	0,50
S7	72,5	120	50	60	0,42	0,50
S8	62,5	120	50	60	0,42	0,50
S9	92,5	80	30	40	0,38	0,50
S10	82,5	80	30	40	0,38	0,50
S11	72,5	80	30	40	0,38	0,50
S12	62,5	80	30	40	0,38	0,50

Table 2 - List of the laser parameters in the first set of pilot prototyping tests

$$v = \frac{d_{spot}}{t_e} \qquad \text{(Eqn. 1).}$$

Fig. 5 – Vectors with 92.5 Watt power

Fig. 6 – Vectors with 82.5 Watt power

Fig. 7 – Vectors with 72.5 Watt power

Fig. 8 – Vectors with 62.5 Watt power

Fig. 9 – Vectors with 92.5 Watt power and 0.5 m/s scanning speed

Fig. 10 – Vectors with 82.5 Watt power and 0.5 m/s scanning speed

Fig. 11 – Vectors with 72.5 Watt power and 0.5 m/s scanning speed

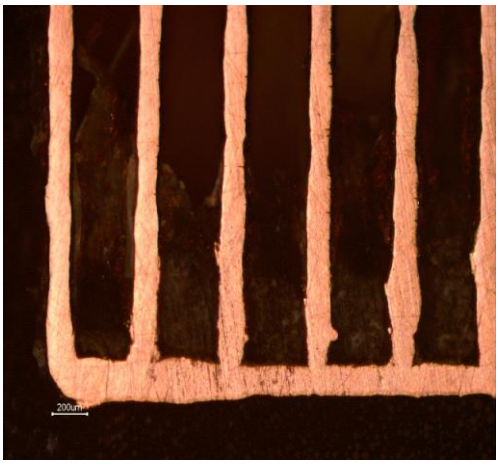

Fig. 12 – Vectors with 62.5 Watt power and 0.5 m/s scanning speed

Fig. 13 – Vectors with 92.5 Watt power and 80 µs laser exposure time

Fig. 14 – Vectors with 82.5 Watt power and 80 µs laser exposure time

Fig. 15 – Vectors with 72.5 Watt power and 80 µs laser exposure time

Fig. 16 – Vectors with 62.5 Watt power and 80 µs laser exposure time

The above set of experiments enabled us to select the optimum combination of laser parameters for obtaining a linear and steady building of the vectors [4, 5]. These parameters will later be used for producing a solid piece with high microstructural quality, i.e. with low gas porosity, low inclusion content and low porosity from incomplete melting of the powder. The optimum set of laser parameters includes a 72.5 W laser power, an exposure time of 120 µs and a spot distance of 40 µm (S3).

These parameters have been applied to obtain a solid piece having a shape similar to the pilot specimen, but with a solid pyramid-shaped base to assist the removal from the building platform and reduce the porosity in the first layers of the piece (Figure 17). That is because in the SLM avoiding porosity in the zone connected to the building platform is an important problem for obtaining a piece fully free from pores.

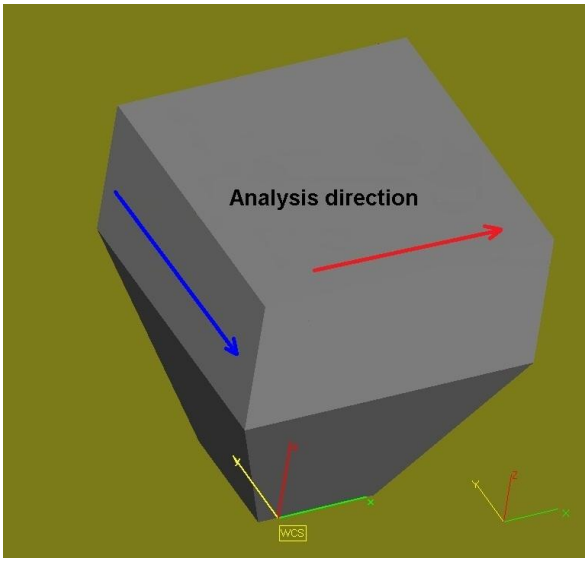

Figure 17 – Model of the solid piece with the directions for roughness evaluation

Obviously, in this case the distance between the vectors (hatches) is lower than in the pilot specimen, to assist contact and joining of the vertical walls, to obtain a solid volume of alloy. The first trial with the selected parameters was carried out with the standard ternary gold alloy (1), that contains only silver and copper additions. The building mode, i.e. the laser path, was comblike, as in the pilot specimen, i.e. a single laser scan for each building layer.

When the distance between the vectors was changed, an important effect was observed, i.e. the persistent presence of pores between adjoining vectors and inside each vector. The amount of porosity can be considerably reduced if the optimum distance is identified, but in all cases porosity tends to be present and can impair the quality of the pieces in the polishing process. Even now the porosity amount obtained after a single laser scan with the best prototyping parameters makes the production of high quality jewellery pieces difficult. Another peculiarity of the solid pieces is given by the fact that porosity is more evident in the inner part of the vectors, while it was nearly absent in the lamellar pieces (Figures 19, 20, 21, 22). The average porosity noticed on the samples built with a single laser scan is equal to 0.19%.

On the other side, the roughness (R_t), as measured on the representative surfaces of the solid piece (Figure 17), shows a typical trend dependent on the direction of the test, i.e. parallel or perpendicular to the direction of the vectors. The roughness of the vertical side is practically independent from the distance between the vectors, while the roughness on the upper side in the direction perpendicular to the vectors increases significantly with the distance between the vectors (Figure 18). This happens because, when the distance between the vectors increases, also the depth of the ridges between the vectors increases.

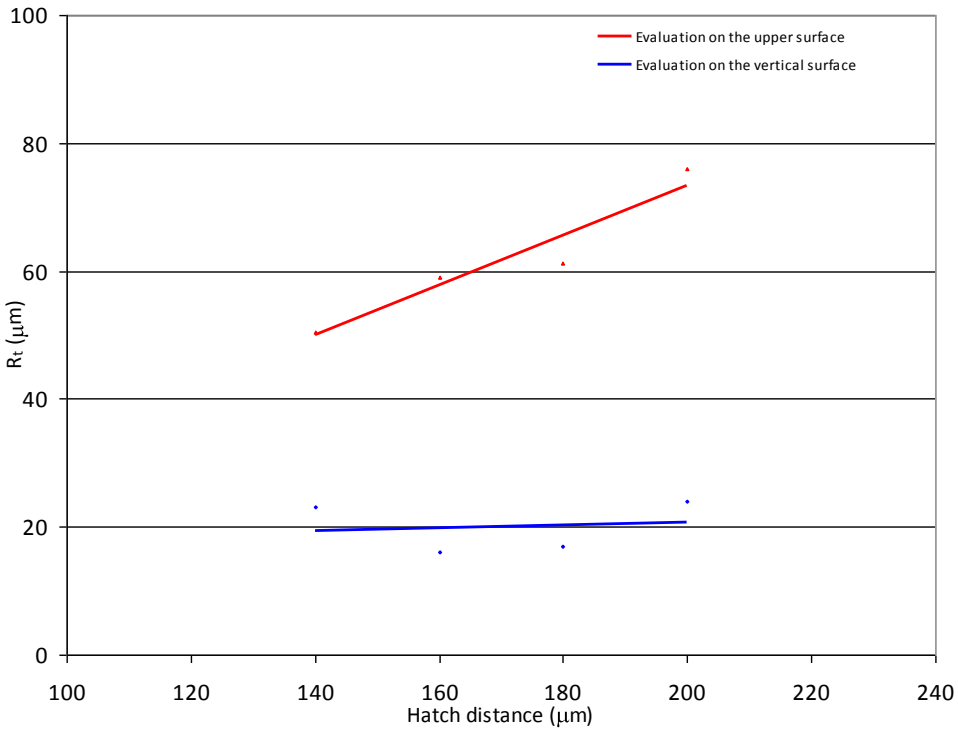

Figure 18 – Roughness R_t as a function of the distance between the vectors on the faces of the solid piece

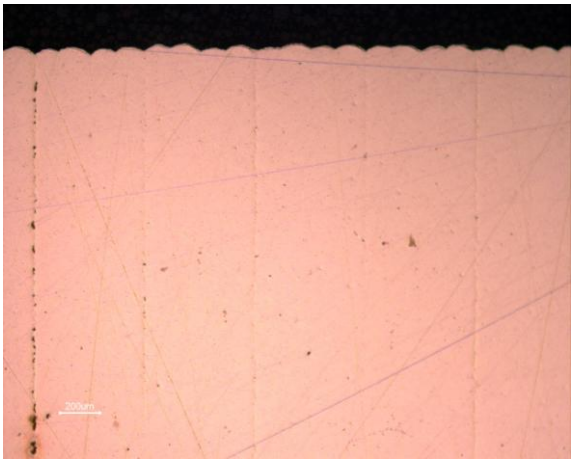

Figure 19 – Cross section of the vectors with 140 µm distance

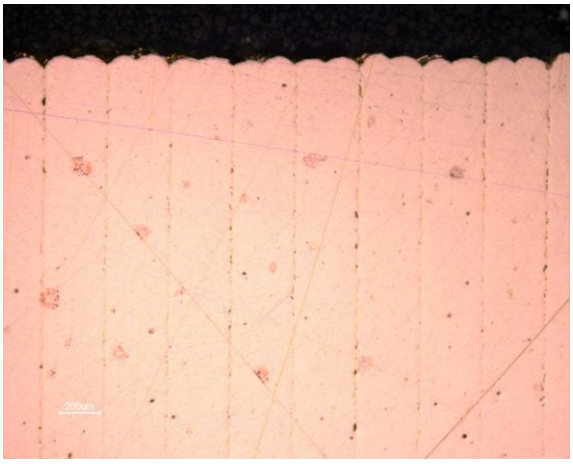

Figure 20 – Cross section of the vectors with 160 µm distance

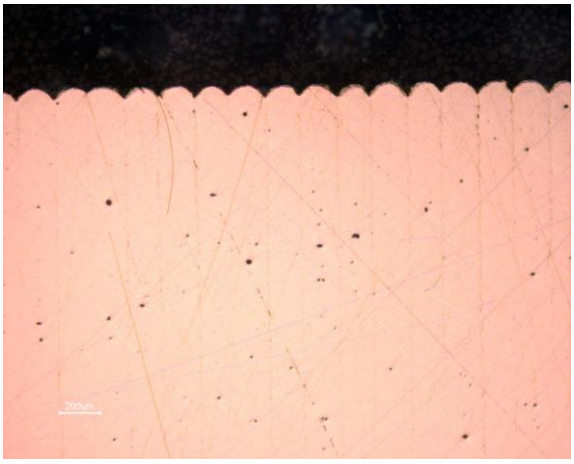

Figure 21 – Cross section of the vectors with 180 µm distance

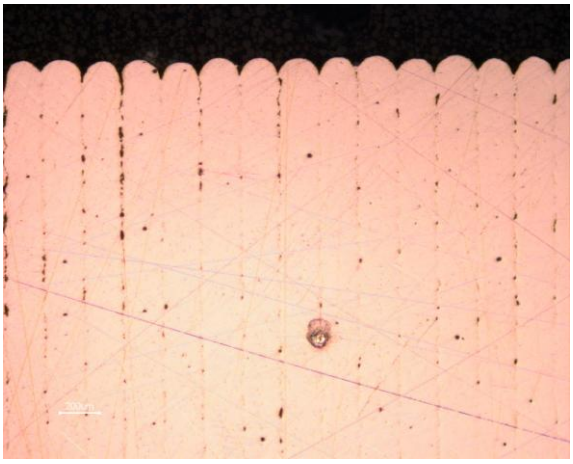

Figure 22 – Cross section of the vectors with 200 µm distance

An attempt to eliminate this residual porosity has been carried out by means of a different prototyping process, i.e. the technique of double laser scan on each building layer of the pieces. With this method a second scan is carried out on the same track of the first scan or between the vectors produced with the first laser scan and on the vectors of the previous scan (Figures 23, 24). The parameters for the second laser scan are similar to the first one and enable to obtain a local re-melting of the alloy between the vectors, to remove the largest part of the defects located in this place.

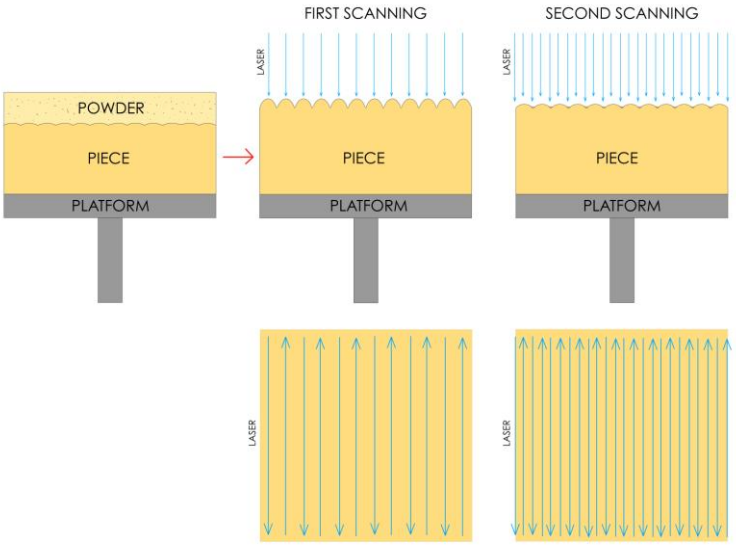

Figure 23 – Schematic representation of a double laser scan

The microstructure obtained after the second scan is very good and residual porosity is reduced to about 0,01% (Figure 25). The interruption of a prototyping test between the first and the second scan on a layer of the piece clearly shows the sealing effect of the second laser scan between the vectors. With a partial re-melting it is possible to remove the internal porosity (Figures 26, 27, 28). The best roughness value after a single scan is 50.6 µm, while after a double scan it is 63.5 µm in the direction perpendicular to the vectors, with a standard alloy (1).

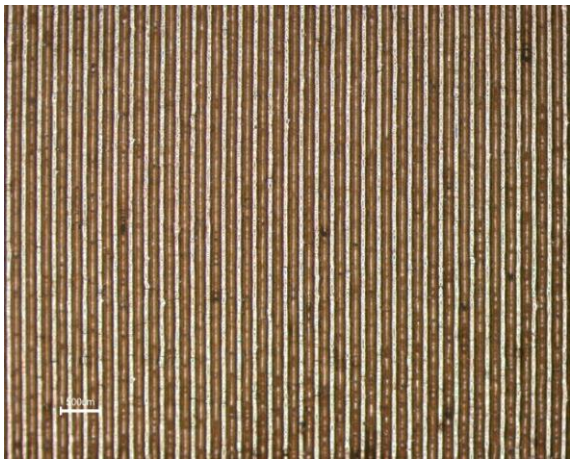

Figure 24 – Upper surface after double laser scan

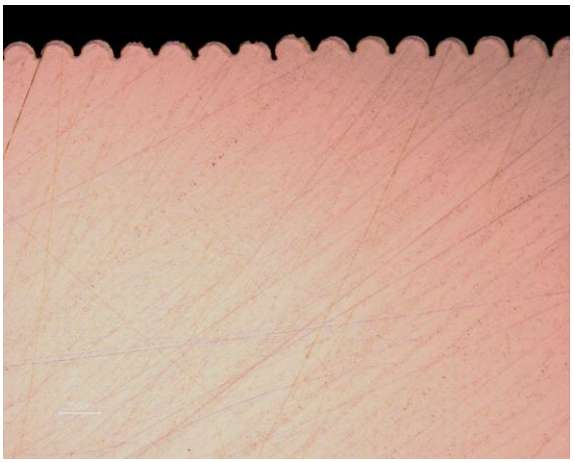

Figure 25 – Metallografic section of the piece with double laser scan

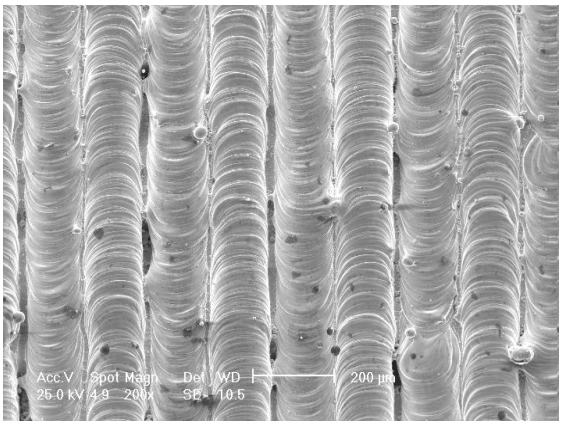

Figure 26 – SEM image before the second scan, with porosity

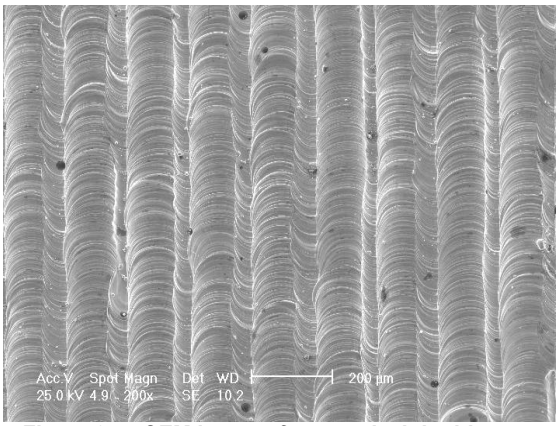

Figure 27 – SEM image after a typical double scan

After identifying the correct combination of laser parameters for obtaining a homogeneous and solid piece with the first gold alloy, the same set of parameters has been used for prototyping the same piece with a different alloy powder (3), containing gallium. Gallium is frequently used in alloys for jewellery production to modify optical, mechanical and thermal properties. Gallium appreciably lowers the melting point of the alloys and significantly changes colour, hardness and surface tension in the molten state.
In fact, solidus temperature of a standard alloy is almost 889°C and liquidus temperature is 901°C, while 2%wt of gallium in the other alloy decreases solidus temperature to 749°C and liquidus temperature to 867°C, with an almost 100°C increase of the melting range.

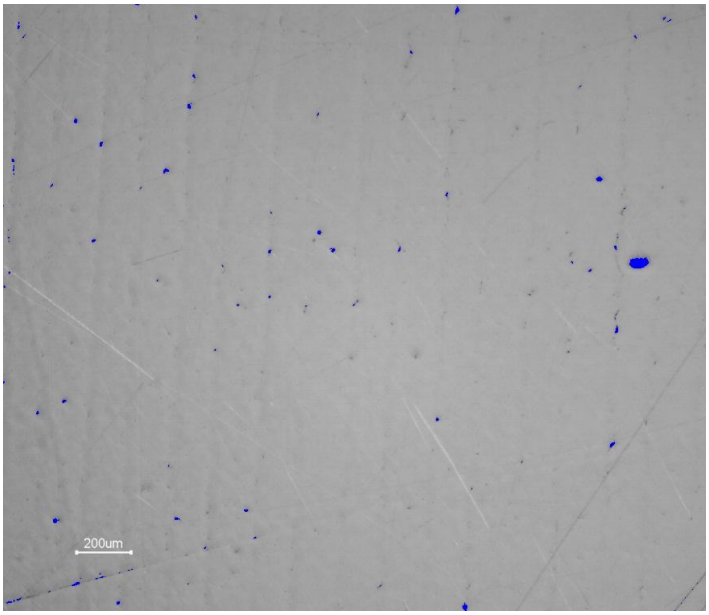

Figure 28 – Example of a digital porosity analysis for a standard alloy (2)

The same set of experiments has been carried out again (Table 1), to find the set of laser parameters more suitable for the gallium containing alloy, but in all cases inner porosity of the pieces and surface roughness (Table 3), measured on the faces in the most representative directions of the piece, were higher, even if the same set of parameters was used that gave the best results with the previous alloy (Figures 29, 30, 31, 32). Moreover the gallium containing alloy shows a higher tendency to eject powder particles on the powder bed, when it is hit by the laser beam. This has an adverse effect on the regular building of the piece (Figure 33). These micro-explosions, with building of large agglomerates of particles on the powder bed, are a contribute to the increase of porosity and to the formation of bulges on the surface of the piece (Figures 34, 35). With the gallium containing alloy (3) pore size is about ten times larger (50 μm) than with the standard ternary alloy (1).

ALLOY	Average porosity (%)	Total roughness (μm)
1	0.01	76.6
2	0.09	84.4
3	0.47	99.1

Table 3. - Average porosity and total roughness after a double laser scan

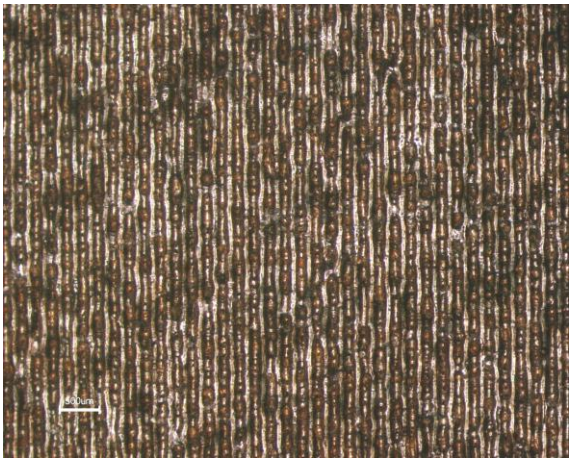

Figure 29 – Surface after double laser scan, gallium containing alloy

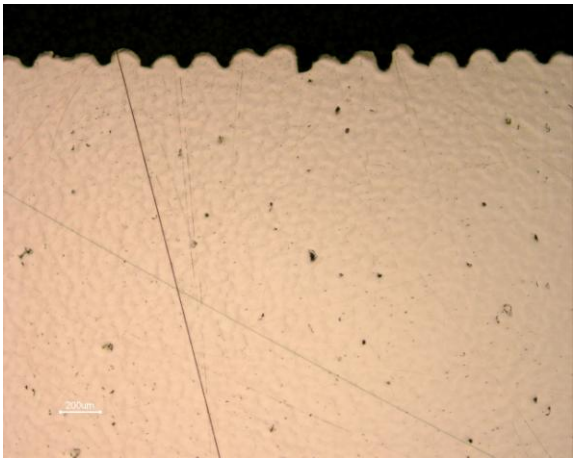

Figure 30 – Metallographic cross section after double laser scan, gallium containing alloy

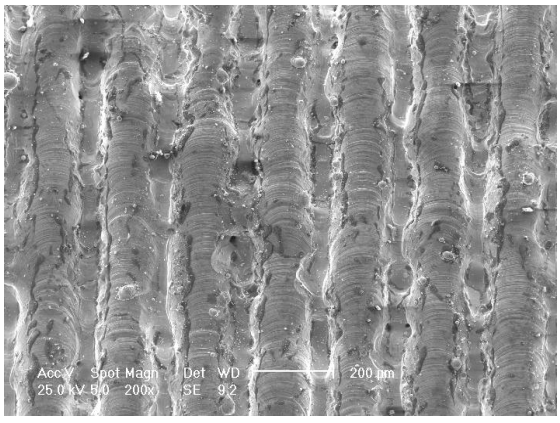

Figure 31 – Double laser scan between the vectors on the gallium containing alloy. SEM image

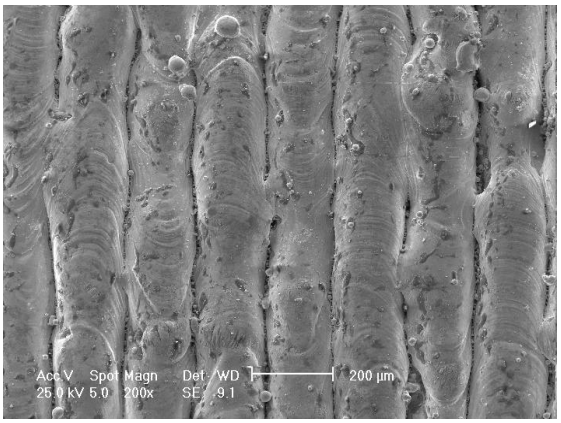

Figure 32 – Single laser scan on the gallium containing alloy. Porosity is present. SEM image

The opposite phenomenon was observed in the pieces produced with traditional or direct investment casting. In the 2%wt Ga alloy porosity is lower (0.05%) than in the gallium free alloy (0.25%). Moreover, in the case of the gallium containing alloy, the pieces produced by traditional investment casting show lower roughness (Figures 36, 37, 38, 39) than the pieces produced by direct investment casting (Table 4). The average roughness (R_t) of the surface of gallium containing alloy pieces along the principal directions (Figure 17) was 15.1 µm for the pieces obtained with traditional investment casting and clearly higher (25.2 µm) for the pieces obtained with direct investment casting.
A minor roughness and porosity of the items with gallium made by investment casting, which are justifiable with the ability of this element to expand during solidification (3.1%) and to wet ceramic surfaces [5], are in contradiction with a higher roughness and porosity of the items produced by selective laser melting.
This phenomena, however, could be associated to a wider melting range which favours a longer liquid phase and the formation of turbulences due to laser scan , beyond gallium effect over the liquidus phase surface tension which tends to produce a tighter vector.

ALLOY	R_t Traditional investment casting (µm)	R_t Direct investment casting (µm)
1	25.0	25.7
3	15.1	25.2

Table 4 – Average roughness for investment cast pieces (wax or resin models)

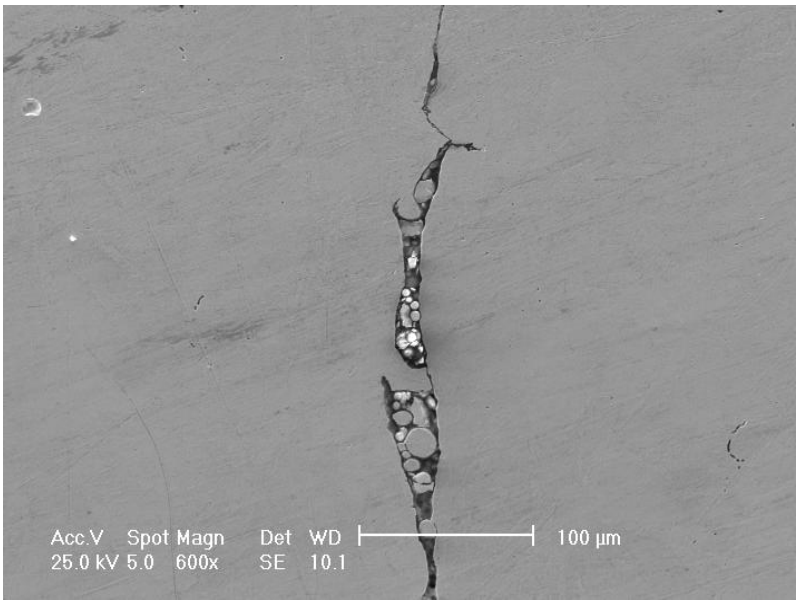

Figure 33 – Build-up of pores and particle clusters in the zone between the vectors

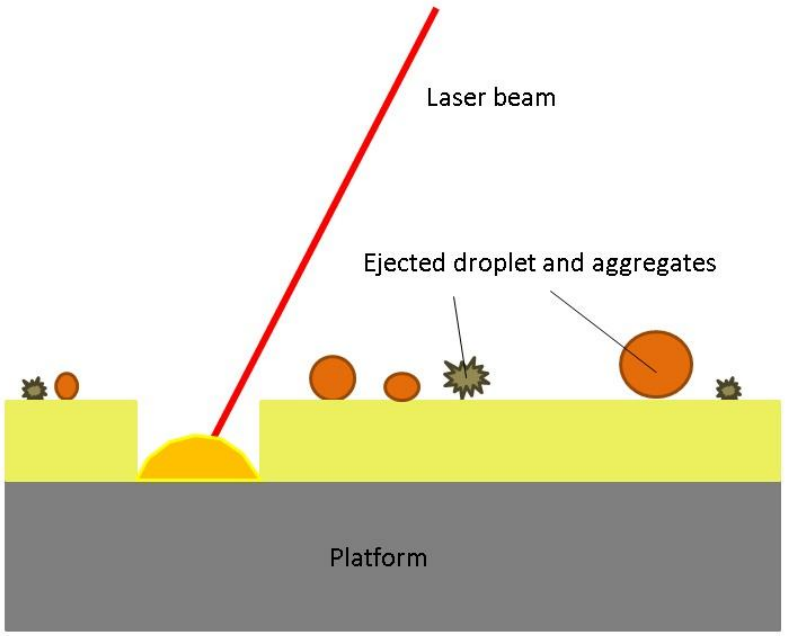

Figure 34 – Starting stage of laser melting with ejection of micro-drops and particle clusters

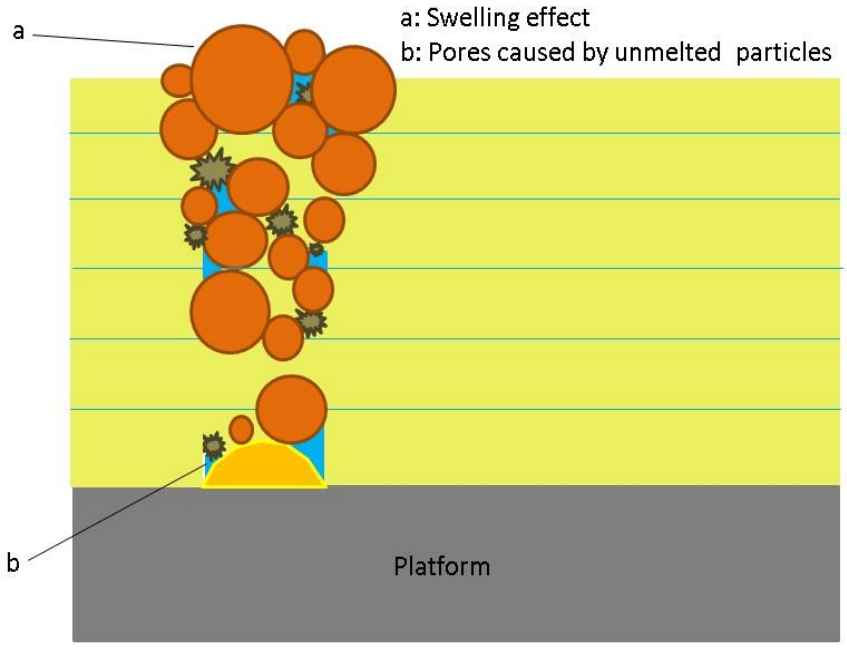

Figure 35 – Final stage of laser melting with formation of porosity and swelling

Figure 36 – Traditional investment casting of the standard alloy (1)

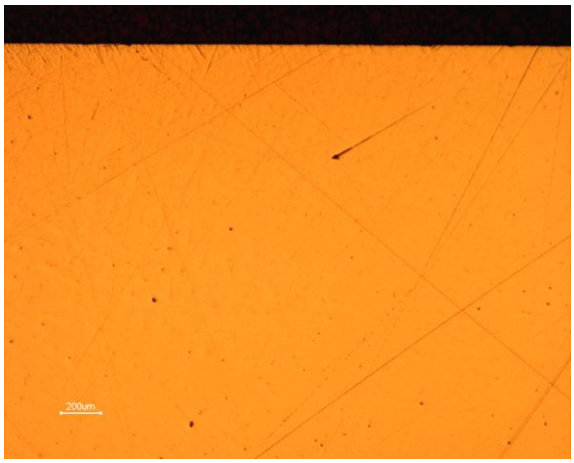

Figure 37 – Traditional investment casting of the gallium containing alloy (3)

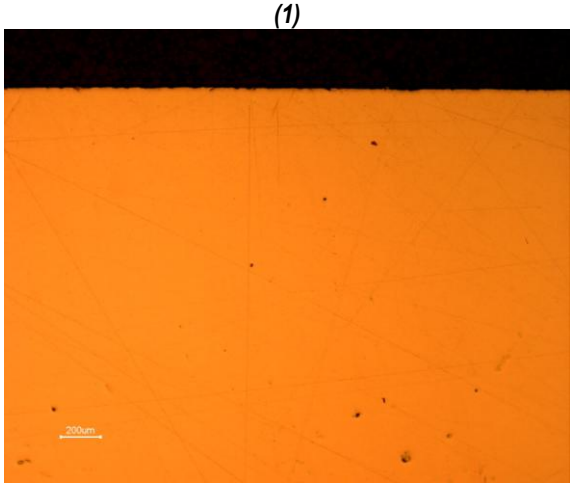

Figure 38 – Direct investment casting of the standard alloy (1)

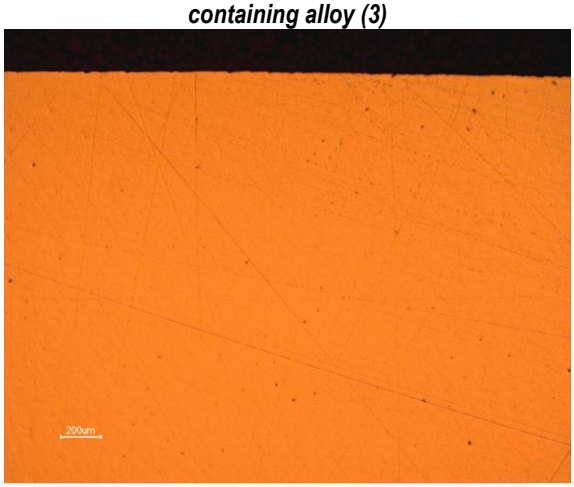

Figure 39 – Direct investment casting of the gallium containing alloy (3)

Particle size distribution of alloy powder particles is another important parameter affecting the quality of the pieces produced with SLM. Usually a powder containing also the finest particles shows higher apparent density, but lower flowability, because of a higher friction among the particles. Such powder gives pieces with lower porosity, but uniform spreading of the powder on the building platform by the blade is more difficult. On the other side, laser parameters and chemical composition being the same, a powder where the finest particles have been removed shows higher flowability and is more easily spread on the building platform (Table 5), but the produced pieces show higher porosity, because of larger cavities that are not fully removed during the fast melting process (Figures 40, 41).

ALLOY	Particle size range (µm)	Flowability - Hall Flowmeter (s/50 g)	Flowability - Carney Flowmeter (s/50 g)	Apparent density (g/cm^3)
1	0-53	18.5	3.5	9.26 ± 0.05
2	5-53	7.4	1.5	9.05 ± 0.03
3	0-53	Not flowing	4.0	8.95 ± 0.04

Table 5 – Flowability and apparent density as a function of particle size range

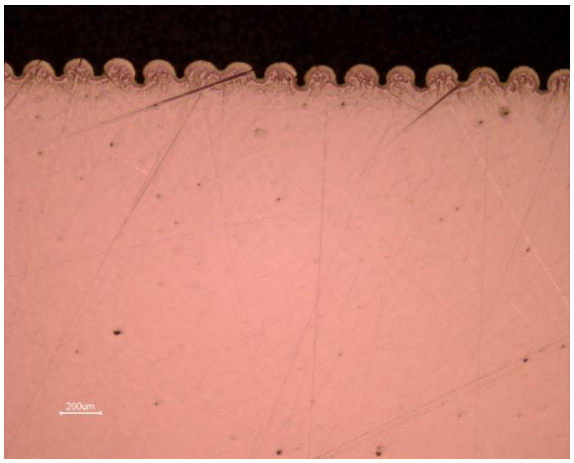

Figure 40 – SLM - Powder with 5–53 µm particle size range

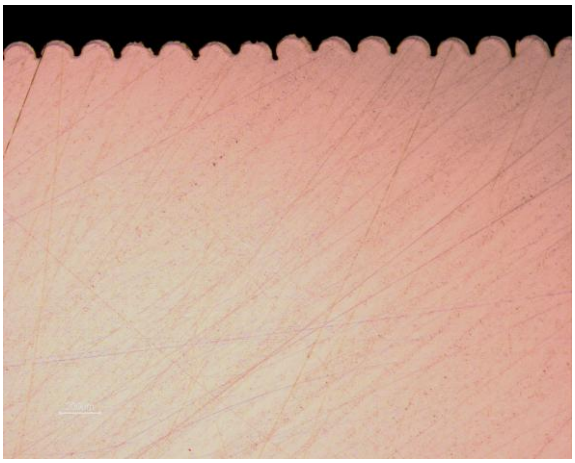

Figure 41 – SLM - Powder with 0-53 µm particle size range

Some high-end elaborate jewellery pieces have been produced to test the set of laser parameters and the double scan process. Such pieces were a hollow ring with round cross section with pierced inner pattern and stone seats (Figure 42, 43, 44, 45) and another hollow ring built with parametric texture. The fist ring was built with a red gold alloy with the composition of the standard alloy (1). For the second ring a yellow gold 3N powder was used (Figures 46, 47, 48). Process parameters used for prototyping both pieces were selected from the previously scrutinized set of parameters.
The result was good. The details of the tri-dimensional model were accurately and consistently reproduced. A good uniformity and precision was observed into the wall thickness, of the ornamental details, holes of the inner pattern and the stone seats. Porosity was very low, even in the connection zone with the support structure.

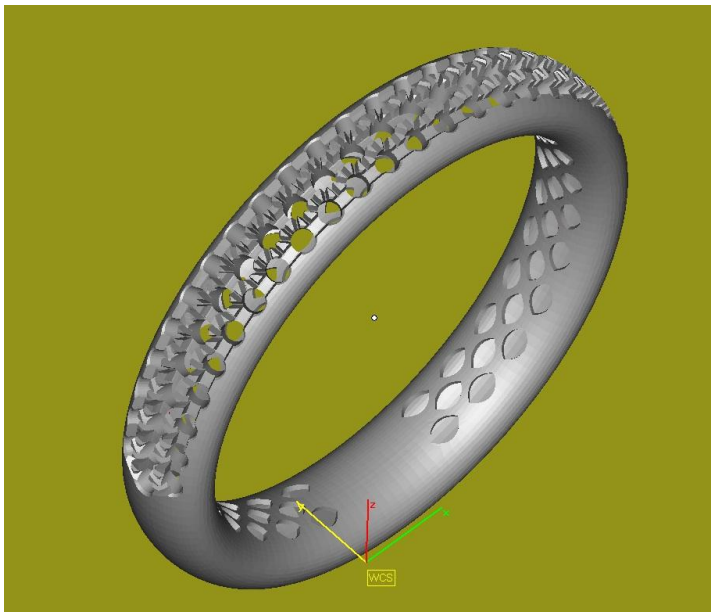

Figure 42 – Tri-dimensional model of the pavé ring obtained with Magics (Materialise)

Figure 43 – Set of pavé rings after completion of the production

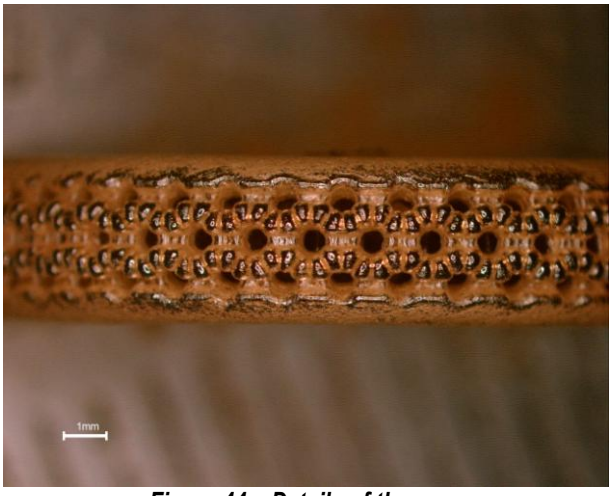

Figure 44 – Details of the pave

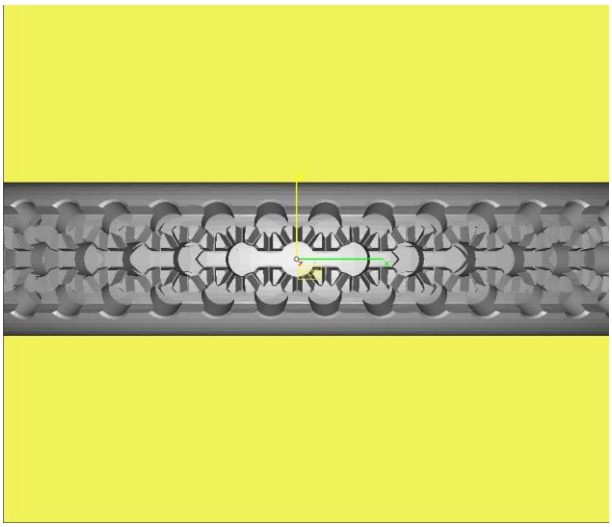

Figure 45 – Details of the pavé model

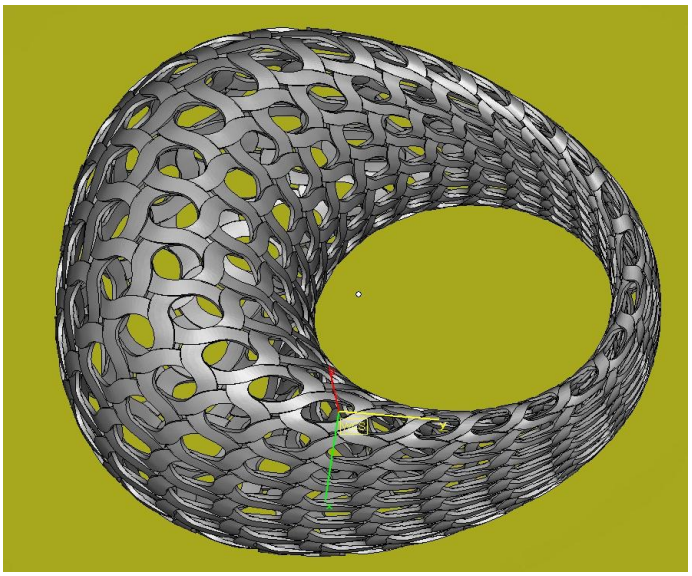

Figure 46 – Tri-dimensional model of the ring with parametric texture obtained with Magics (Materialise)

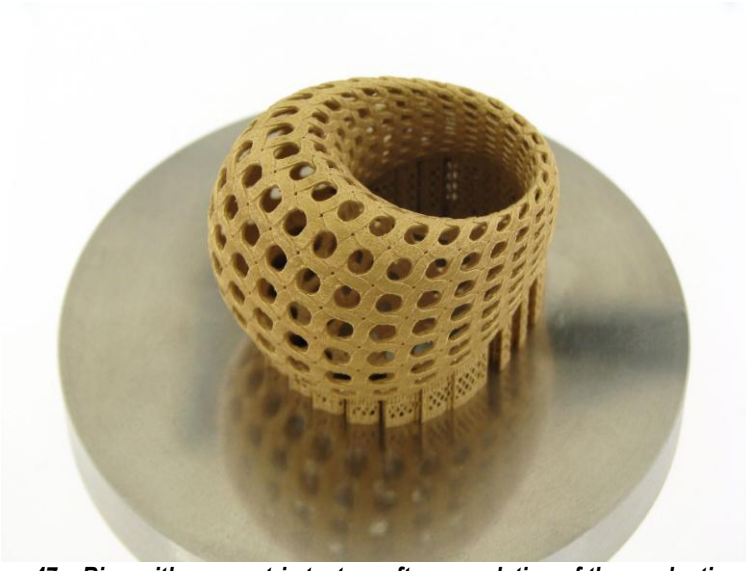

Figure 47 – Ring with parametric texture after completion of the production

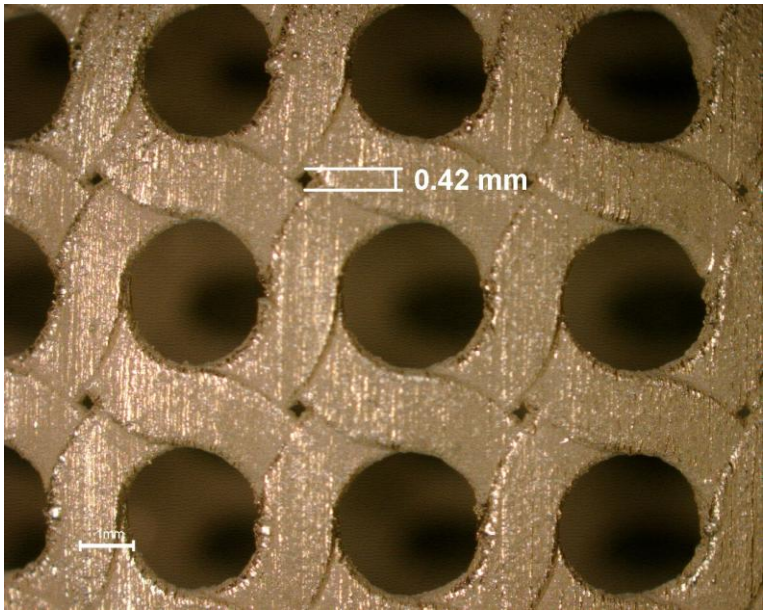

Figure 48 – Detail of the parametric texture

Conclusions

In this new work we examined the possibility of using SLM technique for building jewellery pieces having inner and surface quality similar to pieces produced with investment casting. The feasibility of the SLM method was investigated by means of experiments of increasing complexity, starting from the simplest components, named vectors. Different sets of process parameters were investigated.
After determining the best set of experimental parameters for a single vector, in order to obtain a piece with smooth surface and free from porosity, the same set of parameters was used for building a solid piece formed by a continuous set of vectors. The defects in the produced pieces were evaluated. The reduction of the defects was obtained with an additional laser scan leading to a local re-melting of the alloy, to remove the pores left by the first scan. Our experiments enabled to identify the critical aspects in the use of a gallium containing gold alloy powder. These aspects can be connected with the effect of gallium on the surface tension of the liquid alloy.
The obtained results were implemented for the production of elaborate pieces of high-end jewellery. The results for the accuracy and consistence of the morphological details of the tri-dimensional model were satisfactory with the use of red gold powder and different gold powder colours.

References

1) D. Zito et al., Latest developments in Selective Laser Melting production of gold jewellery, Proceedings of Santa Fe Symposium, 2012 pp. 537-562

2) Kruth, J., Mercelis, P., Froyen, L. and Rombouts, M. (2004), "Binding mechanisms in selective laser sintering and selective laser melting", Proceedings of the Solid Freeform Fabrication Symposium, pp. 44-59

3) Y. Yadroitsev et al., Factor analysis of selective laser melting process parameters and geometrical characteristics of synthesized single tracks, Rapid Prototyping Journal, 3(18)(2012)201-208

4) J. P. Kruth and S. Kumar, Advanced Engineering materials 7(8)(2005)750

5) CRC Handbook of Chemistry and Physics, 87th Edition (2006-2007), David R. Lide editor.